Vol 16 No 11, November 2007
1009-1963/2007/16(11)/3370-07

Chinese Physics

© 2007 Chin. Phys. Soc.
and IOP Publishing Ltd

Modelling of passively Q-switched lasers with intracavity Raman conversion*

Su Fu-Fang(苏富芳)†, Zhang Xing-Yu(张行愚), Wang Qing-Pu(王青圃), Chang Jun(常 军), Jia Peng(贾 鹏), Li Shu-Tao(李述涛), Zhang Xiao-Lei(张晓磊), and Cong Zhen-Hua(丛振华)

School of Information Science and Engineering, Shandong University, Jinan 250100, *China*

(Received 23 February 2007; revised manuscript received 23 March 2007)

We present a model of passively Q-switched Raman lasers by utilizing the rate equations. The intracavity fundamental photon density, Raman photon density and the initial population-inversion density of the gain medium are assumed to be of Gaussian spatial distributions. These rate equations are normalized by introducing some synthetic parameters and solved numerically, and a group of general curves are generated. From these curves we can understand the dependence of the Raman laser pulse characteristics on the parameters about the pumping, the gain medium, the Raman medium and the resonator. An illustrative calculation for a passively Q-switched Nd^{3+}:$GdVO_4$ self-Raman laser is presented to demonstrate the usage of the curves and related formulas.

Keywords: intracavity Raman lasers, passively Q-switched, rate equation, numerical modelling
PACC: 4200, 4255R

1. Introduction

Due to its excellent features, stimulated Raman scattering (SRS) has been widely utilized in many fields.[1−3] Stimulated Raman scattering in crystalline materials is one of the most efficient methods of extending the spectral range of existing lasers.[4−7] Solid state Raman lasers can be realized in a variety of configurations, including single-pass Raman generation,[8] extracavity,[9−11] intracavity Raman resonators,[12−15] or coupled resonators.[16] The intracavity Raman laser has attracted a great deal of attention in recent years because it can reach the much higher intracavity power density and thus operate at a low-threshold, and it often has a high overall conversion efficiency.

The useful tool for analysing the performance of a Q-switched Raman laser is the rate equations, which are based on the conventional Q-switched laser rate equations adding a Raman term and a differential equation of the Raman photon density. The rate equations have been used to model the passively Q-switched Raman lasers in many situations.[17−21] However, because the output pulse properties of the Raman laser depend on quite a lot of parameters about the pumping, gain medium, Raman medium and resonator, it is difficult to obtain the intuitive relations between the output pulse characteristics and the related parameters.

In this paper, we try to make the relations between the output pulse characteristics and the relevant parameters more intuitive by introducing some synthetic parameters. In the rate equations, the Gaussian distributions of the intracavity photon densities of the fundamental and the Raman lasers and the initial population inversion density were taken into account. These space-dependent rate equations of passively Q-switched Raman lasers are normalized by introducing some synthetic parameters and solved numerically, thus a group of general curves are generated. From these curves we can easily understand the dependence of the Raman laser pulse characteristics on the parameters about the pumping, gain medium, Raman medium and resonator. An illustrative calculation for a passively Q-switched Nd^{3+}:$GdVO_4$ self-Raman laser is presented to demonstrate the usage of the curves and the related formulas.

2. Rate equations

The intracavity photon densities are assumed to be of Gaussian spatial distribution for the TEM_{00} mode. Taking the variation of the beam size along

*Project supported by the National Natural Science Foundation of China (Grant No 60478017), the Science and Technology Development Program of Shandong Province, China and the Scientific Research Starting Foundation for Returned Overseas Chinese Scholars, Ministry of Education, China.
†E-mail: sufufang@mail.sdu.edu.cn

the laser axis inside the cavity into consideration, the photon densities of the fundamental laser at the position of the laser and Raman medium are given as

$$\varphi_{\mathrm{L}}(r,t)=\varphi_{\mathrm{L}}(0,t)\exp\Big(-\frac{2r^2}{\omega_{\mathrm{L}}^2}\Big), \tag{1}$$

$$\varphi_{\mathrm{LR}}(r,t)=\varphi_{\mathrm{LR}}(0,t)\exp\Big(-\frac{2r^2}{\omega_{\mathrm{LR}}^2}\Big), \tag{2}$$

where r is the radial coordinate. ω_{L} and ω_{LR} are the beam radii of the TEM_{00} mode at the position of the laser and Raman medium, respectively, and $\varphi_{\mathrm{L}}(0,t)$ and $\varphi_{\mathrm{LR}}(0,t)$ are the fundamental photon densities on the laser axis, respectively. By the continuity of energy flux, we can obtain the relation

$$\omega_{\mathrm{L}}^2\varphi_{\mathrm{L}}(0,t)=\omega_{\mathrm{LR}}^2\varphi_{\mathrm{LR}}(0,t). \tag{3}$$

The Raman photon density at the position of the Raman medium can be expressed as

$$\varphi_{\mathrm{R}}(r,t)=\varphi_{\mathrm{R}}(0,t)\exp\Big(-\frac{2r^2}{\omega_{\mathrm{R}}^2}\Big), \tag{4}$$

where ω_{R} is the beam radius of the Raman laser at the Raman medium, and $\varphi_{\mathrm{R}}(0,t)$ is the Raman photon density on the laser axis at the position of the Raman medium.

We can obtain the rate equations of a passively Q-switched Raman laser by adding a Raman term and a differential equation of the Raman photon density to the rate equations of a passively Q-switched laser[22]

$$\begin{aligned}\int_0^\infty\frac{\mathrm{d}\varphi_{\mathrm{L}}(r,t)}{\mathrm{d}t}2\pi\,r\mathrm{d}r=&\int_0^\infty\frac{2\varphi_{\mathrm{L}}(r,t)}{t_{\mathrm{RT}}}\{\sigma n(r,t)l-\sigma_{\mathrm{g}}n_{\mathrm{S}}(r,t)\,l_{\mathrm{s}}-\sigma_{\mathrm{e}}(n_{\mathrm{S0}}-n_{\mathrm{S}}(r,t))l_{\mathrm{s}}\}2\pi r\mathrm{d}r\\&-\int_0^\infty\frac{2\varphi_{\mathrm{LR}}(r,t)}{t_{\mathrm{RT}}}gh\nu_{\mathrm{R}}c\varphi_{\mathrm{R}}(r,t)l_{\mathrm{r}}2\pi\,r\mathrm{d}r-\int_0^\infty\frac{\varphi_{\mathrm{L}}(r,t)}{t_{\mathrm{RT}}}\Big[\ln\Big(\frac{1}{R_{\mathrm{L}}}\Big)-L_{\mathrm{L}}\Big]2\pi\,r\mathrm{d}r,\end{aligned} \tag{5}$$

$$\begin{aligned}\int_0^\infty\frac{\mathrm{d}\varphi_{\mathrm{R}}(r,t)}{\mathrm{d}t}2\pi\,r\mathrm{d}r=&\int_0^\infty\frac{2\varphi_{\mathrm{R}}(r,t)}{t_{\mathrm{RT}}}gh\nu_{\mathrm{R}}c\varphi_{\mathrm{LR}}(r,t)l_{\mathrm{r}}2\pi\,r\mathrm{d}r\\&-\int_0^\infty\frac{2\varphi_{\mathrm{R}}(r,t)}{t_{\mathrm{RT}}}\{R_{\mathrm{ratio}}\sigma_{\mathrm{g}}n_{\mathrm{S}}(r,t)l_{\mathrm{s}}+R_{\mathrm{ratio}}\sigma_{\mathrm{e}}(n_{\mathrm{S0}}-n_{\mathrm{S}}(r,t))l_{\mathrm{s}}\}2\pi\,r\mathrm{d}r\\&-\int_0^\infty\frac{\varphi_{\mathrm{R}}(r,t)}{t_{\mathrm{RT}}}\Big[\ln\Big(\frac{1}{R_{\mathrm{R}}}\Big)-L_{\mathrm{R}}\Big]2\pi\,r\mathrm{d}r+k_{\mathrm{sp}}\int_0^\infty\varphi_{\mathrm{LR}}(r,t)2\pi\,r\mathrm{d}r,\end{aligned} \tag{6}$$

$$\frac{\mathrm{d}n(r,t)}{\mathrm{d}t}=-\gamma\sigma c\varphi_{\mathrm{L}}(r,t)n(r,t), \tag{7}$$

$$\frac{\mathrm{d}n_{\mathrm{S}}(r,t)}{\mathrm{d}t}=-\frac{S_{\mathrm{l}}}{S_{\mathrm{s}}}\sigma_{\mathrm{g}}c\varphi_{\mathrm{L}}(r,t)n_{\mathrm{S}}(r,t), \tag{8}$$

where $n(r,t)$ is the population-inversion density; $n_{\mathrm{S}}(r,t)$ and n_{S0} are the ground-state and total population densities of the saturable absorber, respectively; σ and l are the stimulated emission cross section and length of the laser medium, respectively; σ_{g} and σ_{e} are the ground-state and excited-state absorption cross sections of the saturable absorber; l_{s} is the length of the saturable absorber; $t_{\mathrm{RT}}=2l_{\mathrm{C}}/c$ is the round-trip transit time of light in the cavity of the optical length l_{C}; c is the speed of light in vacuum; l_{r} is the of length of the Raman medium; g is Raman gain with 1064 nm pump; R_{ratio} is the ratio of absorption cross sections of saturable absorber at laser and Stokes wavelengths; $h\nu_{\mathrm{R}}$ is the photon energy of the Raman laser; k_{sp} is the spontaneous Raman-scattering factor; L_{L} and L_{R} are the remaining round-trip dissipative optical losses at the fundamental wavelength and Raman wavelength, respectively; R_{L} and R_{R} are the output-coupler reflectivities at the fundamental wavelength and Raman wavelength respectively; γ is inversion-reduction factor; S_{l} and S_{s} are the fundamental beam cross-section areas in the laser gain and saturable absorber, respectively.

The initial population inversion density $n(r,0)$ can be expressed as[22]

$$n(r,0)=n(0,0)\exp\Big(-\frac{2r^2}{\omega_{\mathrm{P}}^2}\Big), \tag{9}$$

where ω_{P} is the average radius of the pump beam in the gain medium, and $n(0,0)$ is the initial population-inversion density on the laser axis. The initial value

of $n_{\rm S}(r,t)$ can be considered to be $n_{\rm S0}$.

By utilizing the initial conditions of the $n_{\rm S}(r,t)$ and the $n(r,t)$, substituting expressions (1), (2) and (9) into Eqs.(7) and (8) and integrating the results over time finally, we obtain

$$n(r,t)=n(0,0)\exp\Big(-\frac{2r^2}{\omega_{\rm P}^2}\Big)\exp\Big[-\lambda\sigma c\exp\Big(-\frac{2r^2}{\omega_{\rm L}^2}\Big)\int_0^t\varphi_{\rm L}(0,t)\mathrm{d}t\Big], \tag{10}$$

$$n_{\rm S}(r,t)=n_{\rm S0}\exp\Big[-\frac{S_{\rm l}}{S_{\rm s}}\sigma_{\rm g}c\exp\Big(-\frac{2r^2}{\omega_{\rm L}^2}\Big)\int_0^t\varphi_{\rm L}(0,t)\mathrm{d}t\Big]. \tag{11}$$

Substituting expressions (1)–(4), (10) and (11) into Eqs.(5) and (6) and regrouping the results yield

$$\begin{aligned}\frac{\mathrm{d}\varphi_{\rm L}(0,t)}{\mathrm{d}t}=&\frac{4l\sigma n(0,0)\varphi_{\rm L}(0,t)}{\omega_{\rm L}^2t_{\rm RT}}\times\int_0^\infty\exp\Big[-\gamma\sigma c\exp\Big(-\frac{2r^2}{\omega_{\rm L}^2}\Big)\int_0^t\varphi_{\rm L}(0,t)\mathrm{d}t\Big]\exp\Big[-2r^2\Big(\frac{1}{\omega_{\rm L}^2}+\frac{1}{\omega_{\rm P}^2}\Big)\Big]2r\mathrm{d}r\\&-\frac{4l_{\rm S}n_{\rm S0}\varphi_{\rm L}(0,t)}{\omega_{\rm L}^2t_{\rm RT}}(\sigma_{\rm g}-\sigma_{\rm e})\int_0^\infty\exp\Big(-\frac{2r^2}{\omega_{\rm L}^2}\Big)\exp\Big[-\frac{S_{\rm l}}{S_{\rm s}}\sigma_{\rm g}c\exp\Big(-\frac{2r^2}{\omega_{\rm L}^2}\Big)\int_0^t\varphi_{\rm L}(0,t)\mathrm{d}t\Big]2r\mathrm{d}r\\&-\frac{2gh\nu_{\rm R}cl_{\rm r}\varphi_{\rm L}(0,t)\varphi_{\rm R}(0,t)}{t_{\rm RT}}\frac{1}{1+\omega_{\rm LR}^2/\omega_{\rm R}^2}-\frac{\varphi_{\rm L}(0,t)}{t_{\rm RT}}\Big[\ln\Big(\frac{1}{R_{\rm L}}\Big)+\frac{\sigma_{\rm e}}{\sigma_{\rm g}}\ln\Big(\frac{1}{T_0^2}\Big)+L_{\rm L}\Big],\end{aligned} \tag{12}$$

$$\begin{aligned}\frac{\mathrm{d}\varphi_{\rm R}(0,t)}{\mathrm{d}t}=&\frac{2gh\nu_{\rm R}cl_{\rm r}\varphi_{\rm L}(0,t)\varphi_{\rm R}(0,t)}{t_{\rm RT}}\frac{\omega_{\rm L}^2}{\omega_{\rm R}^2}\frac{1}{1+(\omega_{\rm LR}^2/\omega_{\rm R}^2)}-\frac{4R_{\rm ratio}l_{\rm S}n_{\rm S0}\varphi_{\rm R}\Big(0,t\Big)}{\omega_{\rm R}^2t_{\rm RT}}\Big(\sigma_{\rm g}-\sigma_{\rm e}\Big)\\&\times\int_0^\infty\exp\Big(-\frac{2r^2}{\omega_{\rm R}^2}\Big)\exp\Big[-\frac{S_{\rm l}}{S_{\rm s}}\sigma_{\rm g}c\exp\Big(-\frac{2r^2}{\omega_{\rm L}^2}\Big)\int_0^t\varphi_{\rm L}(0,t)\mathrm{d}t\Big]2r\mathrm{d}r\\&-\frac{\varphi_{\rm R}(0,t)}{t_{\rm RT}}\Big[\ln\Big(\frac{1}{R_{\rm R}}\Big)+R_{\rm ratio}\frac{\sigma_{\rm e}}{\sigma_{\rm g}}\ln\Big(\frac{1}{T_0^2}\Big)+L_{\rm R}\Big]+k_{\rm sp}\varphi_{\rm L}(0,t)\frac{\omega_{\rm L}^2}{\omega_{\rm R}^2},\end{aligned} \tag{13}$$

where T_0 is the small-signal transmission of the saturable absorber

$$T_0=\exp(-\sigma_{\rm g}n_{\rm S0}l_{\rm s}). \tag{14}$$

3. Solutions of the rate equations

By setting $\mathrm{d}\varphi_{\rm L}(0,t)/\mathrm{d}t$ and $\varphi_{\rm R}(0,t)$ to be zero and $t=0$ in expression (10) and using expression (14), we obtain the initial population-inversion density on the laser axis

$$n(0,0)=\frac{\ln(1/R_{\rm L})+\ln(1/T_0^2)+L_{\rm L}}{2\,\sigma\,l}\Big(1+\frac{\omega_{\rm L}^2}{\omega_{\rm P}^2}\Big). \tag{15}$$

Introduce the normalized time τ and the normalized photon densities $\Phi_{\rm L}(r,\tau)$, $\Phi_{\rm R}(r,\tau)$ and N, then we will obtain

$$\tau=\frac{t}{t_{\rm RT}}[\ln(1/R_{\rm L})+\ln(1/T_0^2)+L_{\rm L}], \tag{16}$$

$$\Phi_{\rm L}(r,\tau)=\varphi_{\rm L}(r,\tau)\frac{2\gamma\sigma\,l_{\rm C}}{\ln(1/R_{\rm L})+\ln(1/T_0^2)+L_{\rm L}}, \tag{17}$$

$$\Phi_{\rm R}(r,\tau)=\varphi_{\rm R}(r,\tau)\frac{2\gamma\sigma\,l_{\rm C}}{\ln(1/R_{\rm L})+\ln(1/T_0^2)+L_{\rm L}}, \tag{18}$$

$$N=\frac{\ln(1/R_{\rm L})+\ln(1/T_0^2)+L_{\rm L}}{\ln(1/R_{\rm L})+(\sigma_{\rm e}/\sigma_{\rm g})\ln(1/T_0^2)+L_{\rm L}}. \tag{19}$$

Substituting expressions (16)–(19) into Eqs.(12) and (13) and regrouping the results, we obtain

$$\begin{aligned}\frac{\mathrm{d}\,\Phi_{\rm L}(0,\tau)}{\mathrm{d}\,\tau}=&\,\Phi_{\rm L}(0,\tau)\int_0^1\exp(-Ax^a)\mathrm{d}x\\&-\Big(1-\frac{1}{N}\Big)\Phi_{\rm L}(0,\tau)\frac{1-\exp(-\alpha A)}{\alpha A}\\&-G\,\Phi_{\rm L}(0,\tau)\,\Phi_{\rm R}(0,\tau)-\frac{\Phi_{\rm L}(0,\tau)}{N},\end{aligned} \tag{20}$$

$$\begin{aligned}\frac{\mathrm{d}\,\Phi_{\rm R}(0,\tau)}{\mathrm{d}\,\tau}=&\,G\,\Phi_{\rm L}(0,\tau)\,\Phi_{\rm R}(0,\tau)\beta\\&-R_{\rm ratio}\Big(1-\frac{1}{N}\Big)\Phi_{\rm R}(0,\tau)\Big[\exp(-\alpha A)\\&+\frac{\alpha A}{1+\beta}\int_0^1\exp(-\alpha Ay^{1/(1+\beta)})\mathrm{d}\,y\Big]\\&-\Phi_{\rm R}(0,\tau)L_{\rm rl}+K_{\rm sp}\,\Phi_{\rm L}(0,\tau)\beta,\end{aligned} \tag{21}$$

where

$$x=\exp\Big[-2r^2\Big(\frac{1}{\omega_{\rm L}^2}+\frac{1}{\omega_{\rm P}^2}\Big)\Big], \tag{22}$$

$$a = \frac{1}{1+\omega_{\mathrm{L}}^2/\omega_{\mathrm{P}}^2}, \tag{23}$$

$$y = \exp\Big[-2r^2\Big(\frac{1}{\omega_{\mathrm{L}}^2}+\frac{1}{\omega_{\mathrm{R}}^2}\Big)\Big], \tag{24}$$

$$\beta = \frac{\omega_{\mathrm{L}}^2}{\omega_{\mathrm{R}}^2}, \tag{25}$$

$$A = \int_0^{\tau} \Phi_{\mathrm{L}}(0,\tau)\mathrm{d}\tau, \tag{26}$$

$$\alpha = \frac{\sigma_{\mathrm{g}} S_{\mathrm{l}}}{\gamma\sigma\, S_{\mathrm{s}}}, \tag{27}$$

$$G = \frac{gh\nu_{\mathrm{R}} c l_{\mathrm{r}}}{\gamma\sigma\, l_{\mathrm{c}}} \frac{1}{1+\Big(\omega_{\mathrm{LR}}^2/\omega_{\mathrm{R}}^2\Big)}, \tag{28}$$

$$L_{\mathrm{rl}} = \frac{\ln(1/R_{\mathrm{R}}) + R_{\mathrm{ratio}}(\sigma_{\mathrm{e}}/\sigma_{\mathrm{g}})\ln(1/T_0^2) + L_{\mathrm{R}}}{\ln(1/R_{\mathrm{L}}) + \ln(1/T_0^2) + L_{\mathrm{L}}}, \tag{29}$$

$$K_{\mathrm{sp}} = k_{\mathrm{sp}} \frac{2l_{\mathrm{c}}}{c[\ln(1/R_{\mathrm{L}}) + \ln(1/T_0^2) + L_{\mathrm{L}}]}. \tag{30}$$

Equations (20) and (21) are the very differential equations describing the normalized fundamental and Raman photon densities on the laser axis versus the normalized time. The solutions of Eqs.(20) and (21) are dependent on six synthetic parameters: α, N, β, G, L_{rl} and K_{sp}. The meanings of α and N are the same as those in Ref.[22]; β is the parameter when the spatial variations of the fundamental and Raman intensities are considered; G is the normalized Raman gain coefficient, which is related to the Raman gain coefficient g, the length of the Raman medium l_{r}, the beam cross section area ratio between the fundamental and Raman lasers at the Raman medium, the stimulated emission cross-section σ and the inversion reduction factor γ of the laser medium; L_{rl} is the normalized loss coefficient; K_{sp} is the synthetic parameter that represents normalized spontaneous Raman scattering factor.

By numerically solving Eqs.(20) and (21) in the case of $\omega_{\mathrm{P}} = \omega_{\mathrm{L}}$, we can obtain $\Phi_{\mathrm{R}}(0,\tau)$ for different values of N, α, β, G, L_{rl} and K_{sp}. From the shape of $\Phi_{\mathrm{R}}(0,\tau)$ we can obtain the normalized pulse duration $\Delta\tau$. The real pulse width W is

$$W = \frac{\Delta\tau\, t_{\mathrm{RT}}}{\ln(1/R_{\mathrm{L}}) + \ln(1/T_0^2) + L_{\mathrm{L}}}. \tag{31}$$

The expressions for the peak power output of Raman pulse P_{m} and pulse energy E can be written as

$$P_{\mathrm{m}} = \frac{\pi\omega_{\mathrm{R}}^2 h\nu_{\mathrm{R}}}{4\sigma\gamma\, t_{\mathrm{RT}}}[\ln(1/R_{\mathrm{L}}) + \ln(1/T_0^2) + L_{\mathrm{L}}] \times \ln(1/R_{\mathrm{R}})\,\Phi_{\mathrm{Rm}}, \tag{32}$$

$$E = \frac{\pi\omega_{\mathrm{R}}^2 h\nu_{\mathrm{R}}}{4\sigma\gamma}\ln(1/R_{\mathrm{R}})\,\Phi_{\mathrm{Rinteg}}, \tag{33}$$

where Φ_{Rm} is the maximum value of $\Phi_{\mathrm{R}}(0,\tau)$, and Φ_{Rinteg} is the integral of $\Phi_{\mathrm{R}}(0,\tau)$ over τ from zero to infinity, i.e.

$$\Phi_{\mathrm{Rinteg}} = \int_0^{\infty} \Phi_{\mathrm{R}}(0,\tau)\mathrm{d}\tau. \tag{34}$$

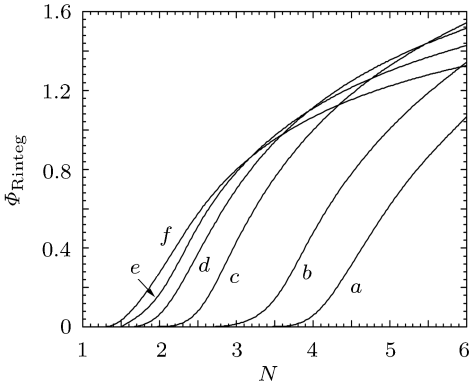


Fig.1. Relation between Φ_{Rinteg} and N for different values of G: 8 (curve a), 10 (b), 15 (c), 20 (d), 25 (e), and 30 (f) with $\beta = 1$ and $L_{\mathrm{rl}} = 0.5$.

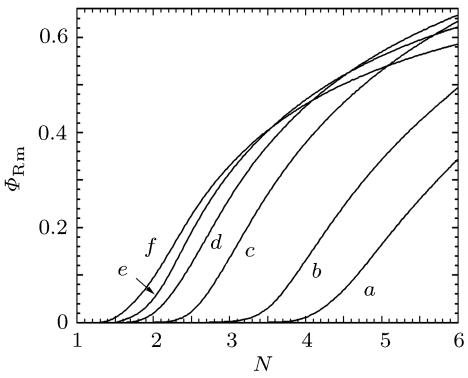


Fig.2. Relation between Φ_{Rm} and N for different values of G: 8 (curve a), 10 (b), 15 (c), 20 (d), 25 (e), and 30 (f) with $\beta = 1$ and $L_{\mathrm{rl}} = 0.5$.

The relations between Φ_{integ}, Φ_{m}, τ of the fundamental laser pulses and α, N, $\omega_{\mathrm{P}}\omega_{\mathrm{L}}$ are given in Ref.[22]. In this paper, we focus on the relations between Φ_{Rinteg}, Φ_{Rm}, τ and N, G, L_{rl}, β. The values of α and K_{sp} in the calculations are 50 and 3×10^{-19}, respectively. Figures 1–3 show the relations of Φ_{Rinteg}, Φ_{Rm}, and τ to the normalized population inversion density N for different values of G with $L_{\mathrm{rl}} = 0.5$ and $\beta = 1$. From Figs.1 and 2 we can see that Φ_{Rinteg} and Φ_{Rm} increase with increasing N. For a given N, there exists an optimal G. With increasing N the normalized time τ decreases first steeply and then slightly. Figures 4–6 show the variations of Φ_{Rinteg}, Φ_{Rm}, and τ with the normalized population inversion density N for different values of L_{rl} with $G = 30$ and $\beta = 1$. For

a given $L_{\rm rl}$, $\Phi_{\rm Rinteg}$ and $\Phi_{\rm Rm}$ increase with increasing N, while τ decreases with increasing N. For a given N, $\Phi_{\rm Rinteg}$ decreases steeply and $\Phi_{\rm Rm}$ decreases slightly with increasing $L_{\rm rl}$, and τ also decreases with increasing $L_{\rm rl}$.

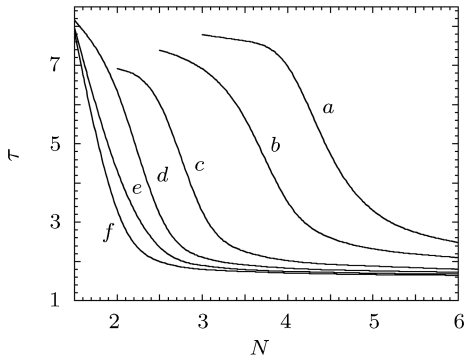


Fig.3. Relation between τ and N for different values of G: 8 (curve a), 10 (b), 15 (c), 20 (d), 25 (e), and 30 (f) with $\beta = 1$ and $L_{\rm rl} = 0.5$.

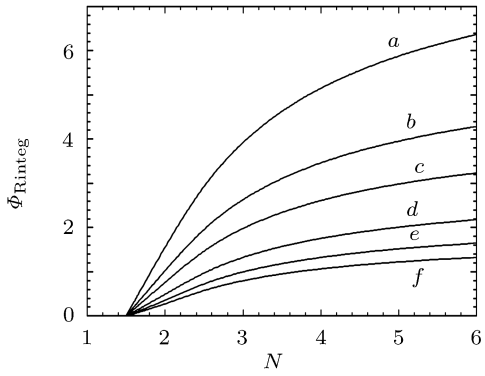


Fig.4. Relation between $\Phi_{\rm Rinteg}$ and N for different values of $L_{\rm rl}$: 0.1 (curve a), 0.15 (b), 0.2 (c), 0.3 (d), 0.4 (e), and 0.5 (f) with $\beta = 1$ and $G = 30$.

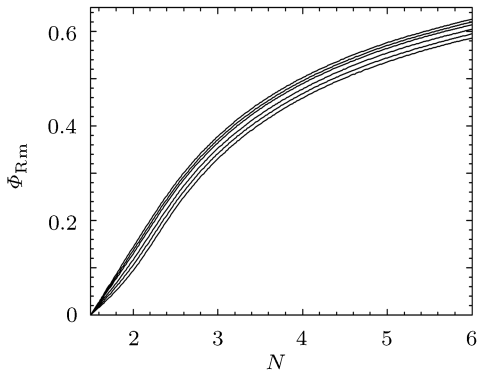


Fig.5. Relation between $\Phi_{\rm Rm}$ and N for different values of $L_{\rm rl}$: 0.1 0.15 , 0.2 , 0.3, 0.4, and 0.5 (from top to bottom) with $\beta = 1$ and $G = 30$.

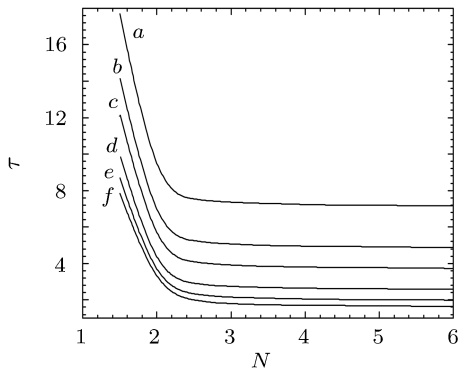


Fig.6. Relation between τ and N for different values of $L_{\rm rl}$: 0.1 (curve a), 0.15 (b), 0.2 (c), 0.3 (d), 0.4 (e), and 0.5 (f) with $\beta = 1$ and $G = 30$.

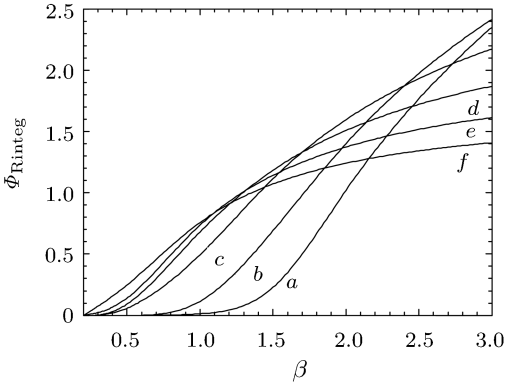


Fig.7. Relation between $\Phi_{\rm Rinteg}$ and β for different values of G: 8 (curve a), 10 (b), 15 (c), 20 (d), 25 (e), and 30 (f) with $N = 3$ and $L_{\rm rl} = 0.5$.

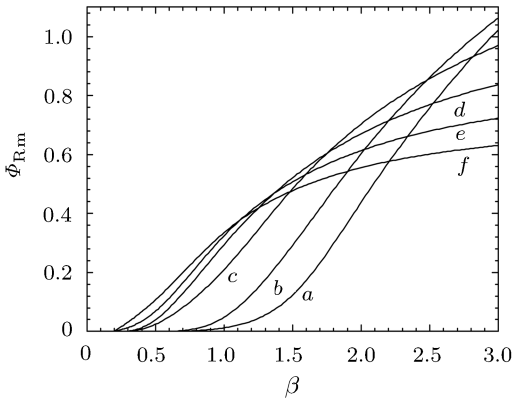


Fig.8. Relation between $\Phi_{\rm Rm}$ and β for different values of G: 8 (curve a), 10 (b), 15 (c), 20 (d), 25 (e), and 30 (f) with $N = 3$ and $L_{\rm rl} = 0.5$.

Figures 7–9 show the variations of $\Phi_{\rm Rinteg}$, $\Phi_{\rm Rm}$, and τ with β for different values of G with $N = 3$. For a given β, there exists an optimal G; for a given G; $\Phi_{\rm Rinteg}$ and $\Phi_{\rm Rm}$ increase with increasing β. Figures 10–12 show the variations of $\Phi_{\rm Rinteg}$, $\Phi_{\rm Rm}$, and τ with β for different values of $L_{\rm rl}$ with $N = 3$. For

a given $L_{\rm rl}$, $\Phi_{\rm Rinteg}$ and $\Phi_{\rm Rm}$ increase with β; for a given β, $\Phi_{\rm Rinteg}$ decreases steeply and $\Phi_{\rm Rm}$ decreases slightly with increasing $L_{\rm rl}$. The trend of τ varying with β is similar to that of τ varying with N.

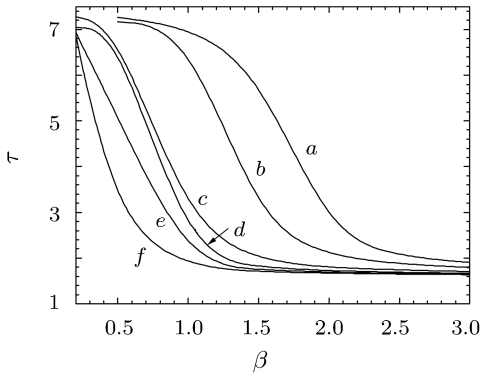


Fig.9. Relation between τ and β for different values of G: 8 (curve a), 10 (b), 15 (c), 20 (d), 25 (e), and 30 (f) with $N = 3$ and $L_{\rm rl} = 0.5$.

4. Applications

Figures 1–12 can help us understand the dependence of the Raman laser pulse characteristics on the ration between the fundamental and the Raman laser mode sizes, the parameter of the gain medium, Raman medium and the resonator. They can also be used to estimate the pulse parameters. We build a fibre-coupled diode end-pumped passively Q-switched Nd:$GdVO_4$ self-Raman laser by using a Cr^{4+}:YAG saturable absorber. The self-Raman laser gain medium is a c-cut 0.5-at% Nd:$GdVO_4$ crystal with a dimension of $3 \times 3 \times 10$ mm^3. Both sides of the Raman crystal are coated for antireflection at 1000–1200 nm. One coated side has a high transmission (90%) at 808 nm. The initial transmission of the 1 mm-long Cr^{4+}:YAG crystal is 0.91. The input mirror is a 300 mm radius-of-curvature concave mirror with high-transmission coating at 808 nm and high-reflection coating at 1000–1200 nm. The output coupler has a high-reflectivity (99.8%) at 1066 nm and a reflectivity of 92.8% at 1176 nm. The overall length of laser cavity is 40 mm. The average radii of the LD pumped beam $\omega_{\rm P}$ and fundamental beam $\omega_{\rm L}$ at the Raman crystal both are 300 μm. The Raman gain of the Nd:$GdVO_4$ crystal is 4.5cm/GW. The round-trip losses of the fundamental and the Raman wavelengths in the cavity are 3.6% and 3.2%, respectively. The inversion-reduction factor is 0.71. The ratio between absorption cross sections of the saturable absorber at the laser and Stokes wavelengths $R_{\rm ratio}$ is 0.2. The ground-state absorption cross section and excited-state absorption cross section of the saturable absorber are 4.3×10^{-18} cm^2 and 8.2×10^{-19} cm^2, respectively.

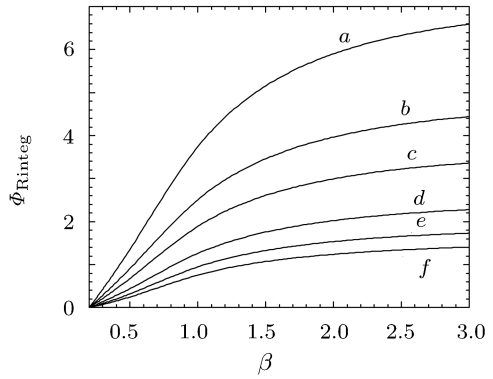


Fig.10. Relation between $\Phi_{\rm Rinteg}$ and β for different values of $L_{\rm rl}$: 0.1 (curve a), 0.15 (b), 0.2 (c), 0.3 (d), 0.4 (e), and 0.5 (f) with $N = 3$ and $G = 30$.

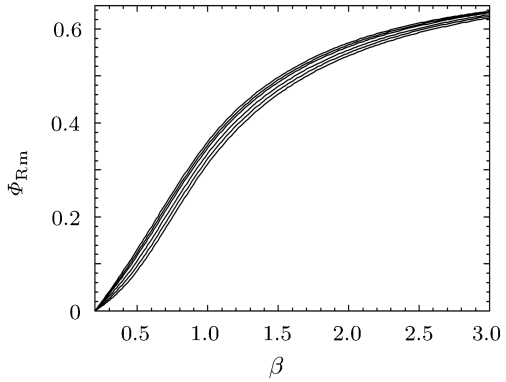


Fig.11. Relation between $\Phi_{\rm Rm}$ and β for different values of $L_{\rm rl}$: 0.1, 0.15, 0.2, 0.3, 0.4, and 0.5 (from top to bottom) with $N = 3$ and $G = 30$.

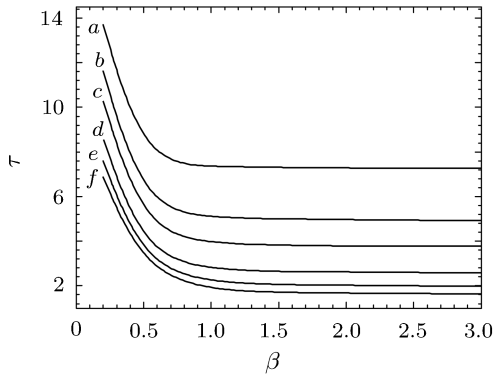


Fig.12. Relation between τ and β for different values of $L_{\rm rl}$: 0.1 (curve a), 0.15 (b), 0.2 (c), 0.3 (d), 0.4 (e), and 0.5 (f) with $N = 3$ and $G = 30$.

The emission cross section of the c-cut Nd:$GdVO_4$ crystal is 1.2×10^{-19} cm^2. By using ABCD matrix we have estimated β and $S_{\rm l}/S_{\rm s}$ to be 0.91 and 1.05, respectively, the spontaneous scattering factor

$k_{\rm sp}$, 2×10^{-10} s^{-1}. By using these values of parameters we can obtain $G = 28$, $N = 2.9$, $L_{\rm rl} = 0.54$, $\alpha = 52$ and $K_{\rm sp} = 2.9 \times 10^{-19}$. From these values we determine $\Phi_{\rm Rinteg}$, $\Phi_{\rm Rm}$, and τ to be 0.59, 0.23 and 2.7, and using expressions (31), (32) and (33) we can obtain the theoretical pulse width, peak power and pulse energy to be 4.8 ns, 4.32 kW and 17.9 μJ respectively. The experimental pulse width, peak power, and pulse energy are found to be 5.2 ns, 3.02 kW, and 15.7 μJ, respectively. These theoretical results are in good agreement with the experimental ones.

5. Conclusions

We have obtained the normalized rate equations for passively Q-switched Raman lasers by introducing some synthetic parameters. These rate equations are solved numerically and a group of general curves describing the relations between $\Phi_{\rm Rinteg}$, $\Phi_{\rm Rm}$, τ and N, G, $L_{\rm rl}$, β are generated. From these curves we can understand the dependence of the laser pulse characteristics on the parameters about the pumping, the Raman medium and the resonator. By these curves and the relevant formulas, we can easily estimate the Raman pulse energy, peak power and pulse width. An illustrative calculation for the passively Q-switched Nd^{3+}:$GdVO_4$ self-Raman laser is presented to demonstrate the usage of the relevant and the relevant formulas. The obtained theoretical results are in agreement with the experimental ones.

References

[1] Zhang X H, Wang Z M and Wan C M 2002 *Acta Phys. Sin.* **51** 1251 (in Chinese)
[2] Wang J and Shi Y M 2006 *Acta Phys. Sin.* **55** 2820 (in Chinese)
[3] Zhang J T 2005 *Chin. Phys.* **14** 169
[4] Pask H M 2003 *Prog. Quantum Electron.* **27** 3
[5] Zverev P G, Basiev T T and Prokhorov A M 1999 *Opt. Mater.* **11** 335
[6] He C and Chyba T H 1997 *Opt. Commun.* **135** 273
[7] Findeisen J, Eichler H J, Peuser P, Kaminskii A A and Hulliger J 2000 *Appl. Phys.* B: *Lasers Opt.* **70** 159
[8] Cerny P and Jelinkova H 2002 *Opt. Lett.* **27** 360
[9] Pask H M, Myers S and Piper J A 2003 *Opt. Lett.* **28** 435
[10] Ding S H, Zhang X Y, Wang Q P, Su F F, Li S T, Fan S Z, Liu Z J, Chang J, Zhang S S, Wang S M and Liu Y R 2005 *Opt. Express* **13** 10120
[11] Ding S H, Zhang X Y, Wang Q P, Su F F, Li S T, Fan S Z, Liu Z J, Chang J, Zhang S S, Wang S M and Liu Y R 2006 *IEEE J. Quantum Electron.* **42** 78
[12] Findeisen J, Eichler H J and Kaminskii A A 1999 *IEEE J. Quantum Electron.* **35** 173
[13] Pask H M and Piper J A 2000 *Opt. Lett.* **36** 949
[14] Pask H M and Piper J A 1998 *Opt. Commun.* **148** 285
[15] Ammann E O 1978 *Appl. Phys. Lett.* **32** 52
[16] Murray J T, Powell R C, Peyghambarian N, Smith D, Austin W and Stolzenberger R A 1995 *Opt. Lett.* **20** 1017
[17] Hamano A, Pleasants S, Okida M, Itoh M, Yatagai T, Watanabe T, Fujii M, Iketaki Y, Yamamoto K and Omatsu T 2006 *Opt. Commun.* **260** 675
[18] Demidovich A A, Apanasevich P A, Batay L E, Grabtchikov A S, Kuzmin A N, Lisinetskii V A, Orlovich V A, Kuzmin O V, Hait V L, Kiefer W and Danailov M B 2003 *Appl. Phys.* B: *Lasers Opt.* **76** 509
[19] Chen W B, Inagawa Y J, Omatsu T, Tateda M, Takeuchi N and Usuki Y 2001 *Opt. Commun.* **194** 401
[20] Loiko Y V, Demidovich A A, Burakevich V V and Voitovich A P 2005 *J. Opt. Soc. Am.* B **22** 2450
[21] Demidovich A A, Voitikov S V, Batay L E, Grabtchikov A S, Danailov M B, Lisinetskii V A, Kuzmin A N and Orlovich V A 2006 *Opt. Commun.* **263** 52
[22] Zhang X Y, Zhao S Z, Wang Q P, Ozygus B and Weber H 2000 *J. Opt. Soc. Am.* B **17** 1166